Journal of Fluorescence (2021) 31:401–414
https://doi.org/10.1007/s10895-020-02671-3

ORIGINAL ARTICLE

Selective and Sensitive ZnO Quantum Dots Based Fluorescent Biosensor for Detection of Cysteine

Umran Duru Kamaci[1] · Musa Kamaci[2]

Received: 15 October 2020 / Accepted: 28 December 2020 / Published online: 7 January 2021

Abstract

In the present article, a novel and effective ZnO quantum dots-based fluorescent probe has been developed for the detection of cysteine in different solutions. Firstly, melamine-based fluorescent pre-probe was successfully synthesized via condensation reaction and, then ZnO quantum dots (QDs) were homogenously dispersed into this solution. This fluorescent probe was used for the detection of cysteine in different solutions such as bovine serum albumin and tap water. ZnO QDs were characterized using XRD, nano-particle size analyzer, and FE-SEM techniques. The size of the ZnO QDs was calculated as 28.03±9.86 nm, and 31.95±10.02 nm from Scherrer's equation and nano-particle size analyzer, respectively. The developed fluorescent probe was exhibited a highly selective and sensitive response to the detection of cysteine. Also, the proposed fluorescent probe has a larger Stokes shift value (236 nm). The limit of detection and linear range of ZnO QDs-based fluorescent biosensor were found as 0.642 μM and 0.1–600 μM, respectively.

Keywords ZnO quantum dots · Biosensor · Cysteine · BSA · Melamine

Introduction

Recently, quantum dots (QDs) have been widely found in various application areas such as biomedical, optoelectronics, molecular recognition, cation/anion detection, protein, and DNA analysis [1–3]. QDs have numerous advantages such as water solubility, biocompatibility, low toxicity, wide emission spectra, low-cost, quantum yield, tunable wavelength, large Stokes shift, ease of modification and preparation compared to the other fluorescence materials [4–7]. A variety of quantum dots (QDs) types such as carbon QDs [8, 9], graphene QDs [10, 11], polymer QDs [12, 13], and metal QDs [14, 15] were prepared to date for the detection of biological compounds such as amino acid [16, 17], DNA [18, 19], and metal ions [20, 21]. Among these various quantum dots types, ZnO QDs have superior properties such as nontoxic and biodegradable nature, an easy synthesis process, and less expensive compared to the other traditional quantum dots types [22]. The prepared ZnO QDs have been used as photodetectors [23], bio-imaging [24], gas sensor [25] applications, and they can also be used as "gate-keepers" to cap the other QDs for fluorescent sensing applications [26]. To the best of our knowledge, they were not used as a fluorescent probe for the detection of cysteine molecules.

Cysteine (Cys) is one of the most important members of low-molecular-weight biological thiols as well as glutathione (GSH) and homocysteine (Hcy) [27]. Although these biological thiols have a similar chemical structure, they are responsible for different biological functions related to various diseases [28]. Cys is of great importance due to its structural composition, redox dynamic balance, physiological functions, control protein function, and signal transduction [29]. An abnormal level of this biological thiol leads to different disorders, symptoms, and diseases such as neurological, skin, lethargy, cardiovascular, slow growth, edema, and psoriasis [30, 31]. Also, insufficient levels of Cys could lead to liver damage, loss of muscle functions, and slow the glow rate in children [32]. Developing an easy, sensitive, and selective fluorescent probe for the detection of this biological small molecule is quite important and it is still needed because of the importance of Cys.

✉ Musa Kamaci
mkamaci@pirireis.edu.tr

Umran Duru Kamaci
umranduru@gmail.com

[1] Faculty of Arts and Sciences, Department of Chemistry, Yildiz Technical University, 34220 Istanbul, Esenler, Turkey

[2] Piri Reis University, 34940 Istanbul, Tuzla, Turkey

In the present paper, a new fluorescence probe was successfully synthesized using syringaldehyde and melamine. Then, ZnO quantum dots (QDs) were homogeneously dispersed into the probe solution by using the ultrasonic probe. The melamine and ZnO QDs-based fluorescent sensor was used for the detection of cysteine in various solutions such as BSA and tap water. Up to now, many kinds of fluorescent chemosensor was developed for the detection of metal ions and biological fluids but a ZnO quantum dot-based fluorescent sensor was developed for the detection of Cysteine in the different solutions for the first time in literature in this paper. The average diameter was calculated as 28.03±9.86, and 31.95±10.02 nm from Scherrer's equation, and nano-particle size analyzer, respectively. The interference effect of the various amino acids, anions, and cations was also studied, and the interference effect of the tested analytes was negligible.

Experimental

Reagents and Materials

Syringaldehyde (SA), melamine (MEL), zinc acetate dihydrate ($Zn(CH_3COO)_2$), sodium hydroxide (NaOH), ethanol (EtOH), glutathione (GSH), L-cysteine (Cys), L-alanine (Ala), L-arginine (Arg), L-aspartic acid (Asp), L-histidine (His), L-homocysteine (Hcy), L-leucine (Leu), L-phenylalanine (Phe), L-proline (Pro), L-tyrosine (Tyr), sodium thiosulfate ($Na_2S_2O_3$), sodium sulfate (Na_3PO_4), sodium acetate ($NaCH_3COO$), disodium hydrogen phosphate (Na_2HPO_4), calcium chloride ($CaCl_2.2H_2O$), potassium chloride (KCl), sodium chloride (NaCl), magnesium chloride ($MgCl_2.6H_2O$), glycine, hydrochloric acid (HCl), tris(hydroxymethyl)aminomethane hydrochloride (Tris), and acetic acid were supplied from Sigma Aldrich and they were used without purification.

Synthesis of AMP

Fluorescent pre-ligand (*4,4',4''-((1E,1'E,1''E)-((1,3,5-triazine-2,4,6-triyl)tris(azanylylidene))tris(methanylylidene))tris(2,6-dimethoxyphenol)* was abbreviated as AMP and it was prepared via condensation reaction of SA (1.640 g, 9 mmol) with MEL (0.378 g, 3 mmol) as in the literature [33–36] and structure of AMP was shown in Fig. 1.

Yield: 98%; **FT-IR (cm^{-1}):** 3133 (-OH), 2972 (aliphatic –CH), 1637 (Imine, -N=CH), 1605–1540 (aromatic –CH); **^{1}H-NMR (400 MHz, DMSO-d_6):** 9.75 (Hydroxyl, -C-O<u>H</u>),8.24 (Imine, -N=C<u>H</u>), 7.19 (Ar-<u>H</u>), 5.95 (Ar-<u>H</u>) and 3.82 (Methoxy, -OC<u>H</u>$_3$); **^{13}C-NMR (100.6 MHz, DMSO-d6):** 191.6 (Hydroxyl, -<u>C</u>-OH), 167.8 (Imine, -N=<u>C</u>H), 148.5 (Ar-<u>C</u>), 142.5 (Ar-<u>C</u>), 127.6 (Ar-<u>C</u>), 107.5 (Ar-<u>C</u>) and 56.5 (Methoxy, -O<u>C</u>H$_3$).

HRMS (EI): Measured values for $C_{30}H_{30}N_6O_9$ (M^+), m/z= 618.218; Theoterical values: m/z= 618.215.

Preparation of ZnO Quantum Dots (QDs)

ZnO quantum dots were prepared via the sol-gel method as follows: 0.55 M $Zn(CH_3COO)_2$ and NaOH solutions were prepared in ethanol/water mixture (1:2, v: v). 40 mL $Zn(CH_3COO)_2$ and 80 mL NaOH solutions were mixed at 60 °C for 6 h, respectively. Then, the mixture was cooled at room temperature and white ZnO precipitated was seen. This precipitate was centrifuged and washed with acetone [37].

Measurements

The crystal structure of ZnO quantum dots was investigated using the Panalytical X'Pert Pro an X-ray diffractometer (Panalytical X'Pert PRO XRD) at room temperature. Nano-particle size analysis of ZnO QDs was carried out using Zetasizer (Malvern Nano ZS) analyzer. FE-SEM image of ZnO QDs was measured using a Field Emission-Scanning Electron Microscopy (FE-SEM, Zeiss EVO LS 10) and the quantum dots sample was coated with a thin layer of gold before SEM measurements. FT-IR spectra of fluorescent pre-probe (AMP), ZnO QDs, fluorescent probe (AMP-ZnO), pristine cysteine (Cys), and cysteine-containing fluorescent probe were recorded using a Thermo Scientific (Nicolet iS10) Spectrophotometer equipped with an ATR unit. Fluorescence measurements were carried out via a Shimadzu (RF-5301PC) fluorescence spectrophotometer, and excitation wavelength and slit width were adjusted as 280 nm and 1.5 nm in all measurements, respectively. Besides, UV-Vis spectra were measured by using a Perkin-Elmer UV-Vis (Lambda 25) spectrophotometer with a double-beam.

Preparation of Stock Solution

The stock solution of AMP (100 μM) was prepared in DMF. 100 μM stock solutions of amino acids (Ala, Arg, Asp, Cys, GSH, Hcy, His, Leu, Phe, Pro and Tyr), anions (CH_3COO^-, HPO_4^{2-}, $PO_4^{3-}$and $S_2O_3^{2-}$), and cations (Ca^{2+}, K^+, Mg^{2+}, and Na^+) were prepared in Britton-Robinson buffer (BR buffer) solution at pH= 7.4. Also, 0.1% ZnO quantum dots were dispersed in an AMP solution by using an ultrasonic homogenizer. pH solutions were prepared in different buffer solutions such as glycine-HCl (pH= 2, and 3), sodium acetate (pH= 4, 5, and 6), and tris-HCl (pH= 7, 8, and 9).

Assay Process

980 μL of BR buffer, 20 μL ZnO quantum dots, 10 μL of the fluorescent pre-probe (AMP), and 10 μL cysteine solution

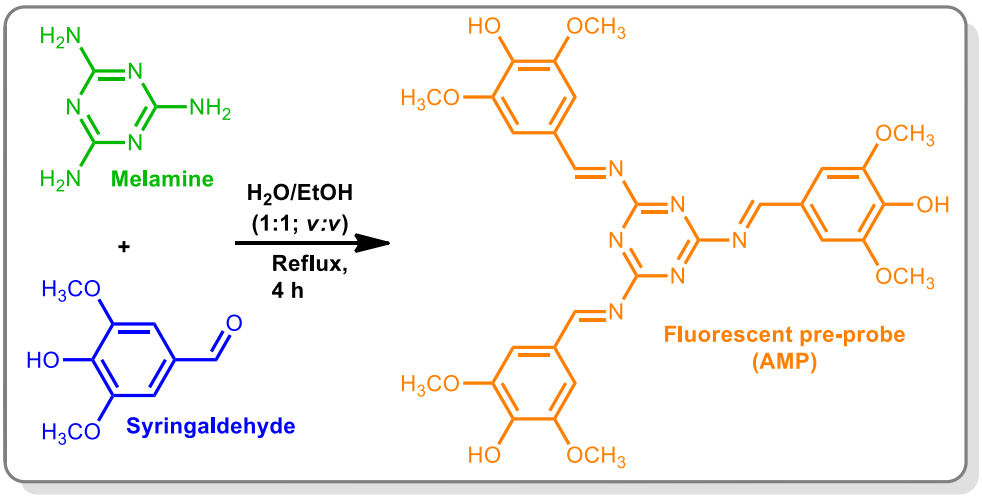

Fig. 1 The synthesis scheme of the fluorescent pre-probe (AMP)

with different concentrations were homogeneously incubated for 15 min and the fluorescence spectra were measured at 280 nm excitation wavelength and 1.5 nm slit width.

Results and Discussion

XRD and SEM Measurements of ZnO Quantum Dots

X-ray diffraction of ZnO quantum dots was measured to investigate the crystal structure of the quantum dots and XRD pattern given in Fig. 2a. ZnO quantum dots have been exhibited the peaks at 2θ= 31.78, 34.48, 36.27, 47.61, 56.73, and 62.92°. Also, the size of the quantum dots was calculated by using Scherrer's equation as follows [38]:

$$d = \frac{k.\lambda}{\beta.cos\theta} \quad (1)$$

where d, k, λ, β, and θ are the size of QDs, constant (0.89), the wavelength of X-ray radiation (0.154 Å), the full width at half maximum, and diffraction angle, respectively. The size of ZnO quantum dots was calculated in the range from 15.77 to 43.92 nm and the average diameter was determined as 28.03 ±9.86 nm. Furthermore, the size of ZnO QDs was determined by using a nano-particle size analyzer, and it was found that the quantum dots have 31.95±10.02 nm the average diameter. These results revealed that the prepared ZnO quantum dots have nanoparticle size. Chen et al. were prepared ZnO quantum dots (QDs) with a hexagonal crystal structure using the sol-gel method and particle size of QDs was found in the range from 16.6 to 32.2 nm [37].

The morphological property of the quantum dots was investigated using an FE-SEM. As displayed in Figs. 2b and c, ZnO quantum dots (ZnO) have a smooth, homogeneously dispersed, and fine surface with a nanoparticle structure.

FT-IR Analysis

FT-IR spectra of the fluorescent pre-probe (AMP), quantum dots (ZnO QDs), fluorescent probe (AMP-ZnO), cysteine (Cys), and AMP-ZnO-Cys were given in Fig. 3. As can be seen in Fig. 3, the characteristic hydroxyl (-OH) stretching vibration of AMP was recorded at 3133 cm^{-1}. –NH, aliphatic –CH (Al-CH), and imine (-N=CH) stretching vibrations of fluorescent pre-probe were seen at 3454, 3374, 2960, and 1637 cm^{-1}, respectively [35]. In the FT-IR spectrum of ZnO quantum dots (ZnO), four strong peaks were observed at 3376, 1402, 827, and 685 respectively, due to –OH, and Zn-O stretching vibrations [39, 40]. In the structure of the fluorescent probe (AMP-ZnO), imine (-N=CH), hydroxyl (-OH), Al-CH, and Zn-O stretching vibrations were observed at 1644, 3422, 2930, 1380, 850, and 652 cm^{-1}, respectively. According to the FT-IR spectrum of Cys, hydroxyl (-OH), Al-CH, anti-symmetric $–CH_2$, and asymmetric –COO stretching vibrations were recorded at 3125, 2975, 2911, 1585 cm^{-1}, respectively [41]. Imine (-N=CH), hydroxyl (-OH), Al-CH, anti-symmetric $–CH_2$, asymmetric –COO, and Zn-O stretching vibrations in the structure of AMP-ZnO-Cys were also seen at 1640, 3399, 2930, 2875, 1418, 1382, 865, and 661, respectively. The stretching vibration values in the structure of AMP-ZnO were shifted after the addition of Cys due to the formation of strong hydrogen bonding between Cys and the fluorescent probe.

Optical and Fluorescence Properties

The photophysical properties of AMP, ZnO, and AMP-ZnO were investigated by measuring the absorption and emission spectra of these materials in the presence and absence of cysteine (Cys) using UV-Vis and fluorescence spectrophotometers. UV-Vis spectra of these compounds were displayed in Fig. 4a and UV-Vis measurements were taken after the

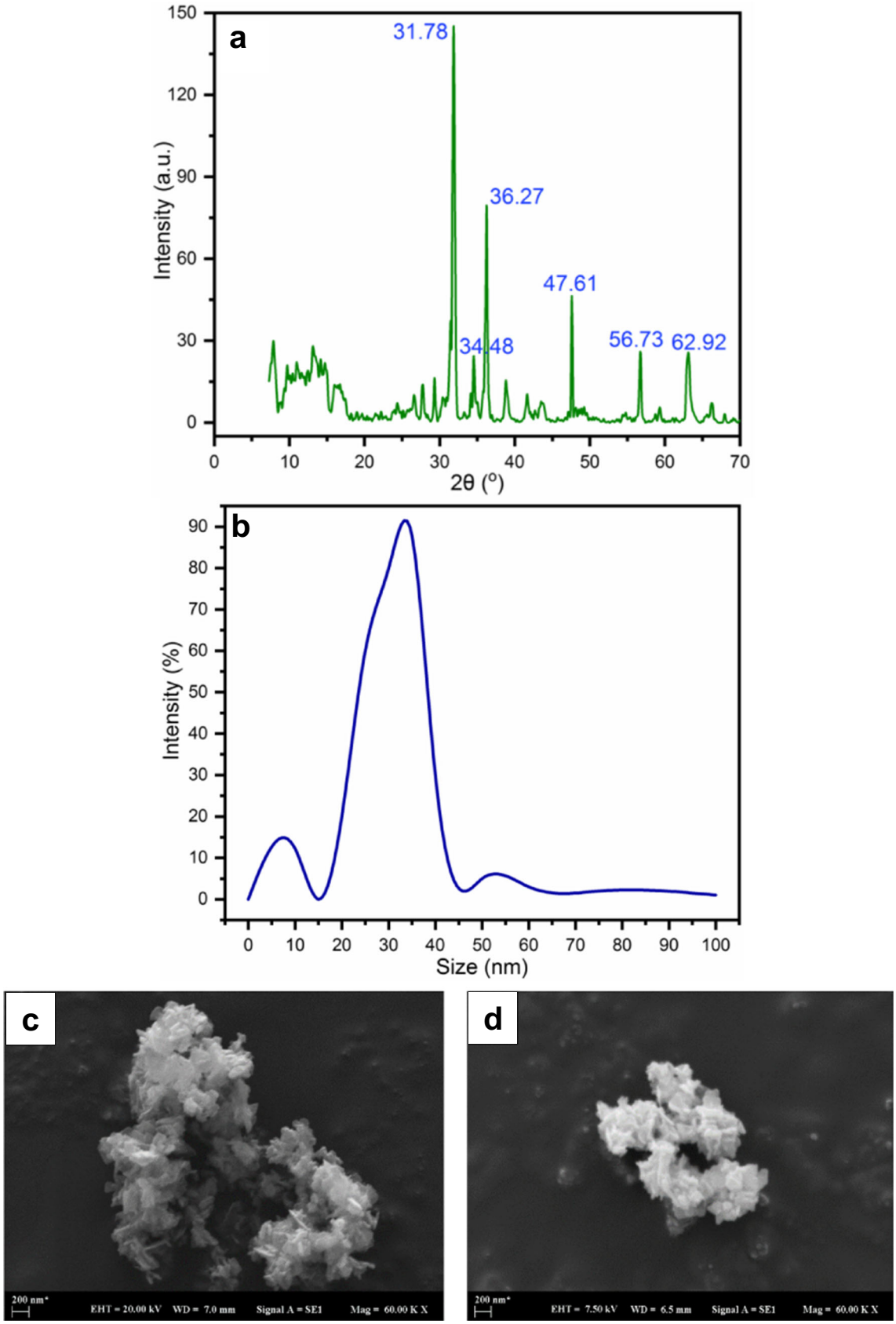

Fig. 2 XRD pattern (**a**), zeta analysis (**b**), and SEM image (**c**, **d**) of ZnO quantum dots

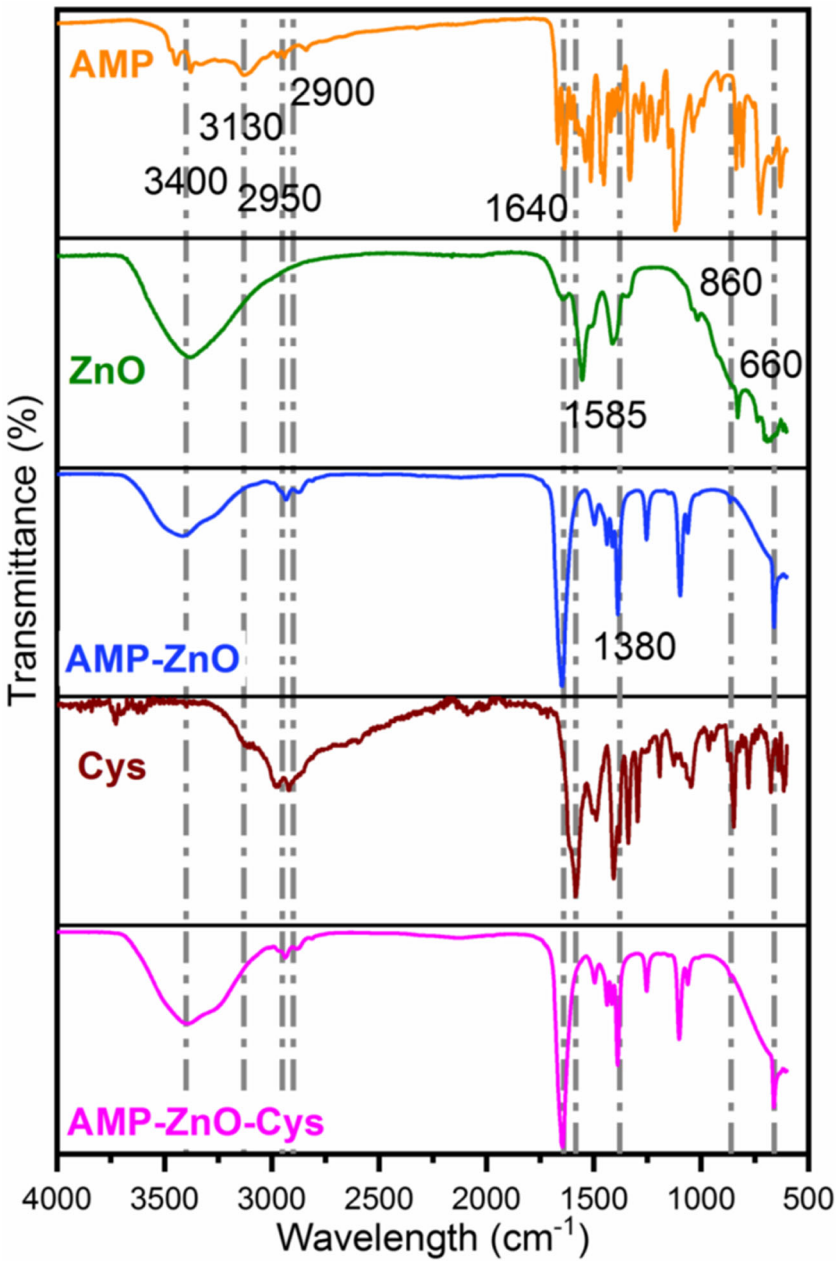

Fig. 3 FT-IR spectra of AMP, ZnO QDs, cysteine (Cys), AMP-ZnO, and AMP-ZnO-Cys

solutions incubated for 15 min. As can be seen in Fig. 4a, AMP, and ZnO quantum dots have only one absorption band at 341 and 351 nm, respectively. When mixed these two solutions (AMP and quantum dots, 1:2, *v: v*), the absorbance band was observed at 355 nm. Moreover, the absorption band of the AMP-ZnO mixture in the presence of Cys was observed at 377 nm. The wavelength of the fluorescent probe and AMP-ZnO-Cys mixture was exhibited to a red-shift change and the absorption band of AMP-ZnO-Cys was shifted about 20 nm compared to the fluorescent probe. Figure 4b shows fluorescence emission spectra of AMP, ZnO, AMP-ZnO, and AMP-ZnO-Cys. These measurements were carried out by homogeneously incubating the solution for 15 min Also, slit width and excitation wavelength were adjusted as 1.5 nm and 280 nm in these measurements, respectively. According to Fig. 4b, AMP, and ZnO QDs were showed only one strong emission intensity around 428, and 464 nm, respectively. When mixed AMP and ZnO quantum dots (1:2, *v: v*), the fluorescence intensity of the fluorescent probe was seen at 482 nm. With the addition of the cysteine in the fluorescent probe solution, fluorescent intensity was observed at 516 nm. The emission wavelength of the fluorescent probe and AMP-ZnO-Cys mixture was exhibited to a hypsochromic (red) change and the wavelength of AMP-ZnO-Cys was shifted about 34 nm compared to the fluorescent probe. The reason for a red-shift change in both UV-Vis and fluorescent

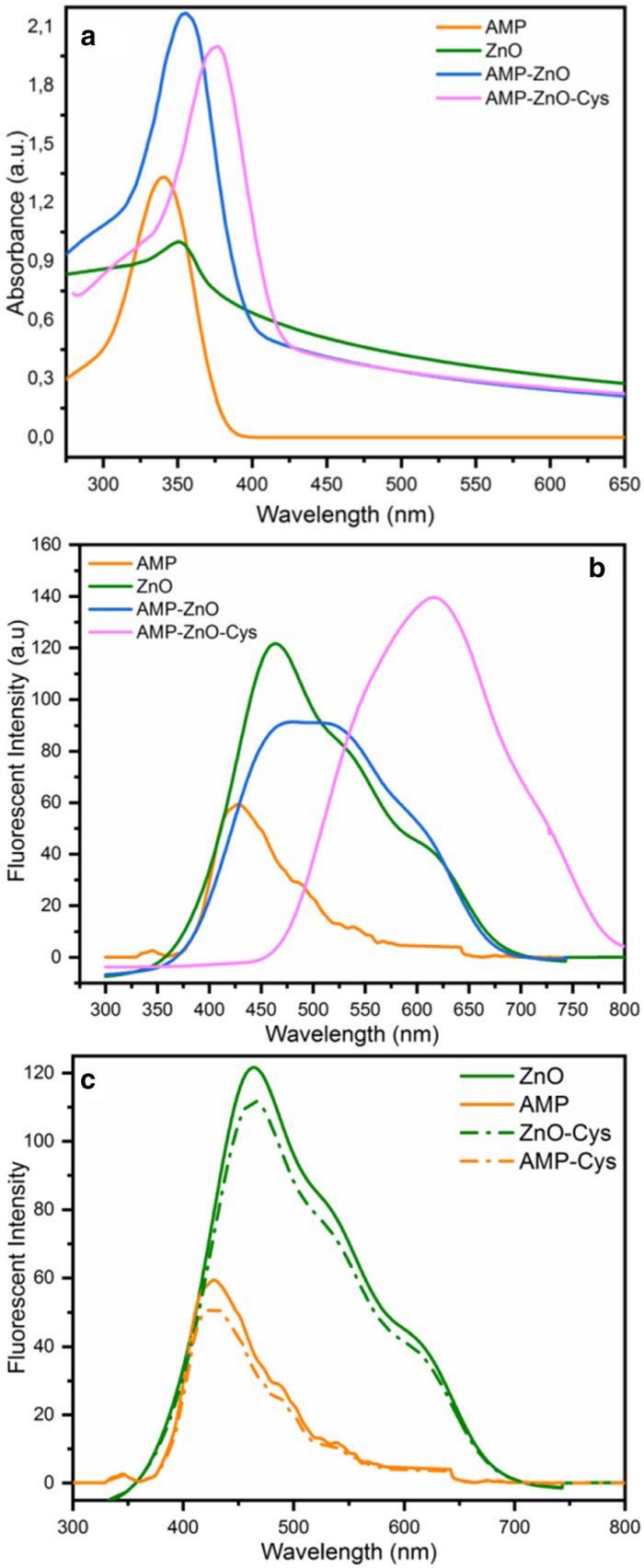
a
AMP
ZnO
AMP-ZnO
AMP-ZnO-Cys
Absorbance (a.u.)
Wavelength (nm)
b
AMP
ZnO
AMP-ZnO
AMP-ZnO-Cys
Fluorescent Intensity (a.u)
Wavelength (nm)
c
ZnO
AMP
ZnO-Cys
AMP-Cys
Fluorescent Intensity
Wavelength (nm)

◀ **Fig. 4** UV-Vis (**a**) and fluorescence (**b**, **c**) spectra of alone AMP and ZnO quantum dots in the presence and absence of cysteine

measurements was the formation of new hydrogen bonding between the fluorescent probe and cysteine molecules [42]. Besides, with the addition of ZnO QDs in the fluorescent pre-probe (AMP) solution AMP-ZnO system has been exhibited much stronger emission intensity. The Stokes shift ($\Delta\lambda_{ST}$) value of the fluorescent probe and AMP-ZnO-Cys mixture was determined as 202 and 236 nm, respectively [43]. These results demonstrated that ZnO quantum dots-based fluorescent probe and AMP-ZnO-Cys mixture have remarkable a large $\Delta\lambda_{ST}$ value.

The fluorescent spectra of alone AMP and ZnO QDs in the presence and absence of Cys were recorded to explain the selectivity of the developed fluorescent chemosensor (Fig. 4c). As can be seen in Fig. 4c, the fluorescence intensity of both AMP and ZnO QDs were a bit increased in the presence of Cys. It was observed that neither AMP nor ZnO QDs were exhibited any interference effect on the developed sensor.

pH and Incubation Time Effect

The emission spectra were measured at the different pH media to investigate the interaction of the ZnO quantum dots-based fluorescent probe with cysteine molecules. pH effect is one of the important parameters for the detection of biological molecules [44] and it was affected the determination of Cys due to different functional groups such amine (-NH_2), carbonyl (-C=O), and thiol (-SH) as of this biological small biothiol [45]. The pH effect on fluorescence intensity was given in Fig. 5a. These measurements were carried out using 100 μM cysteine and the pH value of the solution was adjusted using different buffer solutions such as glycine-HCl (pH= 2, and 3), sodium acetate (pH= 4, 5, and 6), and tris-HCl (pH= 7, 8, and 9). The fluorescence intensity value of the fluorescent probe in the presence of Cys was determined as 7.51, 9.10, 10.70, and 58.18 at acidic pH solutions (pH= 3, 4, 5, and 6). At a neutral medium (pH= 7), fluorescence intensity was measured as 137.93. Also, the fluorescent intensity was determined between 59.18 and 17.08 at alkaline pH solutions (pH= 8, 9, 10, 11, and 12). As can be seen in these results, the ZnO quantum dots-based fluorescent probe has the highest fluorescence intensity at a neutral medium due to the protonation or deprotonation of the functional groups in the structure of the fluorescent biosensor and cysteine [46]. Rad et al. stated that the only carboxyl group in the structure of Cys is protonated at neutral pH and the net charge of the compound is zero [47]. These results indicated that the proposed fluorescent probe was compatible with the physiological and biological environment of the human body and this pH value was selected as the experimental value.

Incubation time was another important parameter due to adequate and good interaction between cysteine and ZnO QDs-based fluorescent probe. The incubation time effect was displayed in Fig. 5b and these measurements were carried out in the presence of 980 μL of BR buffer, 20 μL ZnO QDs, 10 μL of the fluorescent pre-probe (AMP), and 10 μL Cys solutions at room temperature and pH= 7.0. The emission intensity value was gradually increased in the range from 5 to 15 min and it was continuously decreased after 15 min. These results revealed that the proposed sensor has a maximum emission intensity when incubated for 15 min and this incubation time was taken as the experimental value.

The Selectivity of the Fluorescent Probe

To evaluate the selectivity of ZnO quantum dots-based fluorescent sensor, emission intensity was measured in the presence of the various analytes such as amino acids (Ala, Arg, Asp, Cys, GSH, Hcy, His, Leu, Phe, Pro and Tyr), anions (CH_3COO^-, HPO_4^{2-}, $PO_4^{3-}$and $S_2O_3^{2-}$), and cations (Ca^{2+}, K^+, Mg^{2+}, and Na^+). These measurements were carried out in the presence of 980 μL of BR buffer, 20 μL ZnO quantum dots, 10 μL of the fluorescent probe (AMP), and 10 μL analytes (Fig. 6) at pH= 7.0 after 15 min incubation. The emission intensities of Cys, Hcy, and GSH were found as 139.62, 48.15, 46.07 a.u. at 516 nm, respectively. Among the tested analytes, the emission intensities of cation, anions, and the other amino acids were determined in the range 16.73 to 26.46 a.u., 9.90 to 16.00 a.u., and 15.23 to 41.88 a.u., respectively. These emission intensity results clearly indicated that the proposed ZnO QDs-based fluorescent probe was exhibited a highly selective and strong fluorescence response toward cysteine. The distinction of the emission intensity values between cysteine and the other analytes (cations, anions, and amino acids) was still clearly obvious and the effect of the other amino acids, anions, and cations on fluorescence intensity is negligible. Besides, Cys has approximately 3-fold more emission intensity value compared to Hcy, and GSH. Besides, the proposed fluorescent sensor was clearly distinguished by these small biological thiols (Cys, Hcy, and GSH) between each other.

Detection of Cysteine

To determine the limit of detection and linear response range of the fluorescent probe, fluorescent intensity was measured in the presence of 980 μL of BR buffer, 20 μL ZnO quantum dots, 10 μL of AMP, and different cysteine concentrations (10–600 μM) at room temperature and pH= 7.0 after 15 min incubation (Fig. 7a). Fluorescent intensity of the ZnO QDs-based probe was perpetually increased in the range from 0.1 to 600 μM Cys concentrations. It was found that the

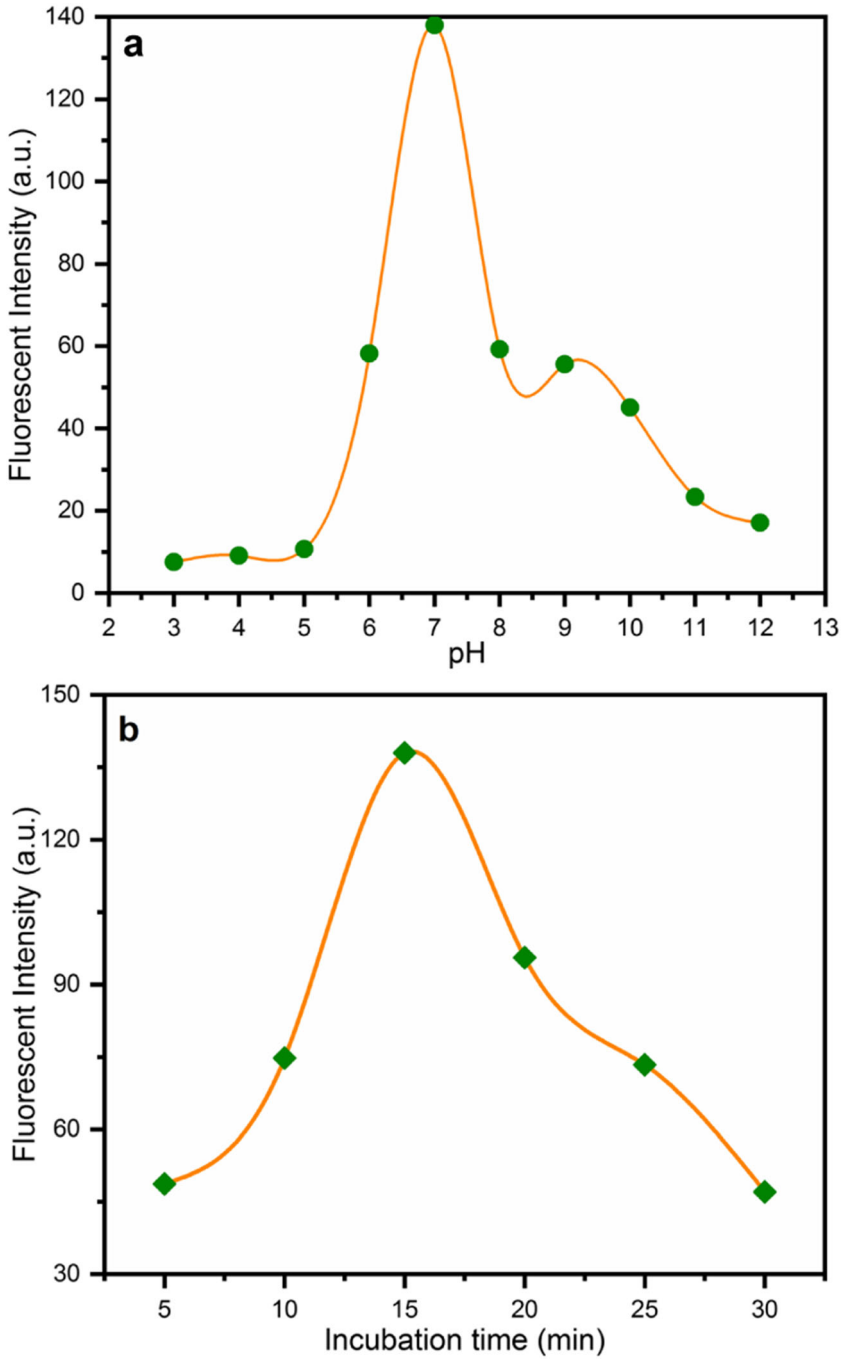

Fig. 5 pH (**a**) and incubation time (**b**) effect on fluorescent intensity

fluorescence intensity of the ZnO QDs-based biosensor was increased with increasing Cys concentration.

The limit of the detection (LOD) value of ZnO quantum dots-based fluorescent sensor was calculated using the fluorescence titration method as the following Eq. 2 [48, 49]:

$$\mathrm{LOD} = \frac{3.\sigma_{bi}}{m}$$

where m and σ_{bi} (0.063) are the slope of the graph obtained from Fig. 7a and the standard deviation of blank measurement. The regression equation for the fluorescent biosensor was found as F= 0.2942[Cys] (μM) + 105.34 with good linearity (R^2=0.9967). The fluorescence intensity was proportionally increased in the range from 0.1 μM and 600 μM, and these concentrations range was determined as a linear range of the biosensor. The limit of detection value (LOD) value of the ZnO-QDs-based fluorescent sensor was also calculated as 0.642 μM.

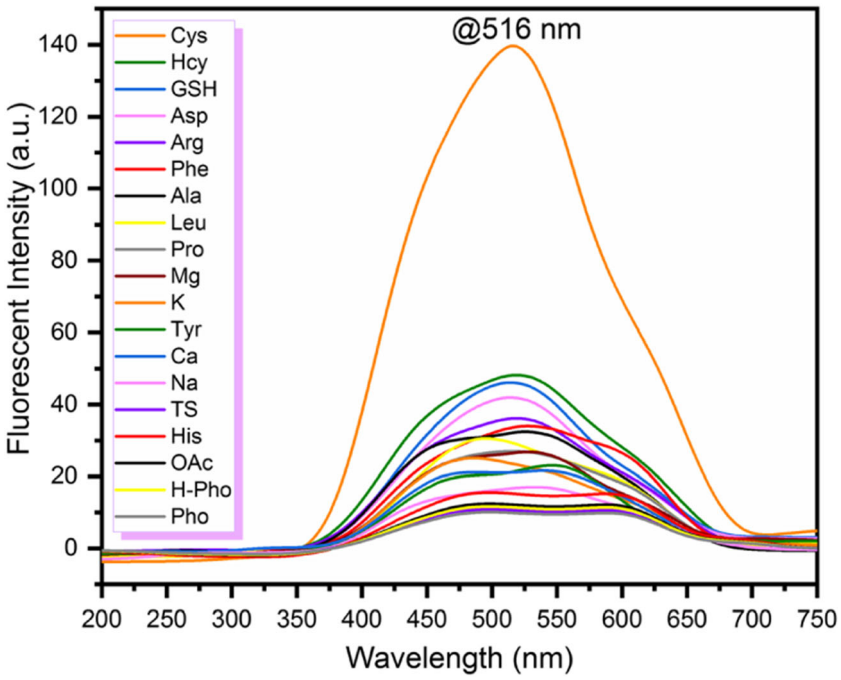

Fig. 6 The selectivity of the ZnO quantum dot-based fluorescent sensor toward Cys

The Selectivity of ZnO QDs-Based Fluorescent Probe

The interference effect is an important parameter to evaluate the performance of the developed fluorescent sensor. The interference effect of the various analytes such as amino acids (Ala, Arg, Asp, Cys, GSH, Hcy, His, Leu, Phe, Pro and Tyr), anions (CH_3COO^-, HPO_4^{2-}, $PO_4^{3-}$and $S_2O_3^{2}$), and cations (Ca^{2+}, K^+, Mg^{2+}, and Na^+) was investigated in the presence of 980 μL of BR buffer, 20 μL ZnO quantum dots, 10 μL of AMP and 10 μL 100 μM analyte at room temperature and pH= 7.0 after 15 min incubation (Fig. 8). According to Fig. 8, the other analytes were not changed the fluorescence intensity of AMP-ZnO-Cys system, and the proposed biosensor has been exhibited a high selectivity to Cys. Also, Hcy has been not exhibited any interference effect on the biosensor.

The proposed ZnO QDs-based fluorescent sensor was compared with the other studies in the literature to investigate LOD and linear range values of the developed sensor and the results were summarized in Table 1. As mentioned above, ZnO quantum dots were generally used in gas sensor, photodetector, and bio-imaging applications and they can also be used as "gate-keepers" to cap the other QDs for fluorescent sensing applications. The developed biosensor could not be compared with the other studies due to ZnO QDs are not used in a study for the detection of cysteine yet. Therefore, the ZnO QDs-based biosensor was only compared to the other quantum dots sensor that developed for cysteine detection with various methods such as chemiluminescence, colorimetric, electrochemical, fluorometric, and fluorescence. The developed sensor was exhibited a relatively wide linear range compared to the other studies [32, 47, 50–53]. Also, the LOD value of the developed biosensor is comparable with the other studies.

Photostability

The photostability of AMP-ZnO and AMP-ZnO-Cys was studied in BR buffer at pH= 7.0 for 60 min (Fig. 9.) As can be seen in Fig. 9, the emission intensities of the biosensor in the absence and presence of the cysteine were decreased around 10, and 5% for AMP-ZnO and AMP-ZnO-Cys, respectively. These results showed that AMP-ZnO and its Cys complex were exhibited good photostability.

Analytical Application

The developed ZnO QDs-based biosensor was examined in different sample solutions such as the lower (10 μM), medium (300 μM), and higher (600 μM) test concentrations of bovine serum albumin (BSA, 0.1 mg/mL) and tap water to investigate the practicability of the fluorescent sensor (Table 2). As can be seen in Table 2, the recoveries were determined in the range from 99.7 to 100.7 for BSA solutions and 100.8 to 101.3 for tap water samples, respectively. Also, the relative standard deviation (RSD, n=3) was found between 1.17 and 2.46%. These results demonstrated that the ZnO QDs-based fluorescent sensor for the detection of cysteine could be successfully applied in analytical application with satisfied, reliable, and practical results.

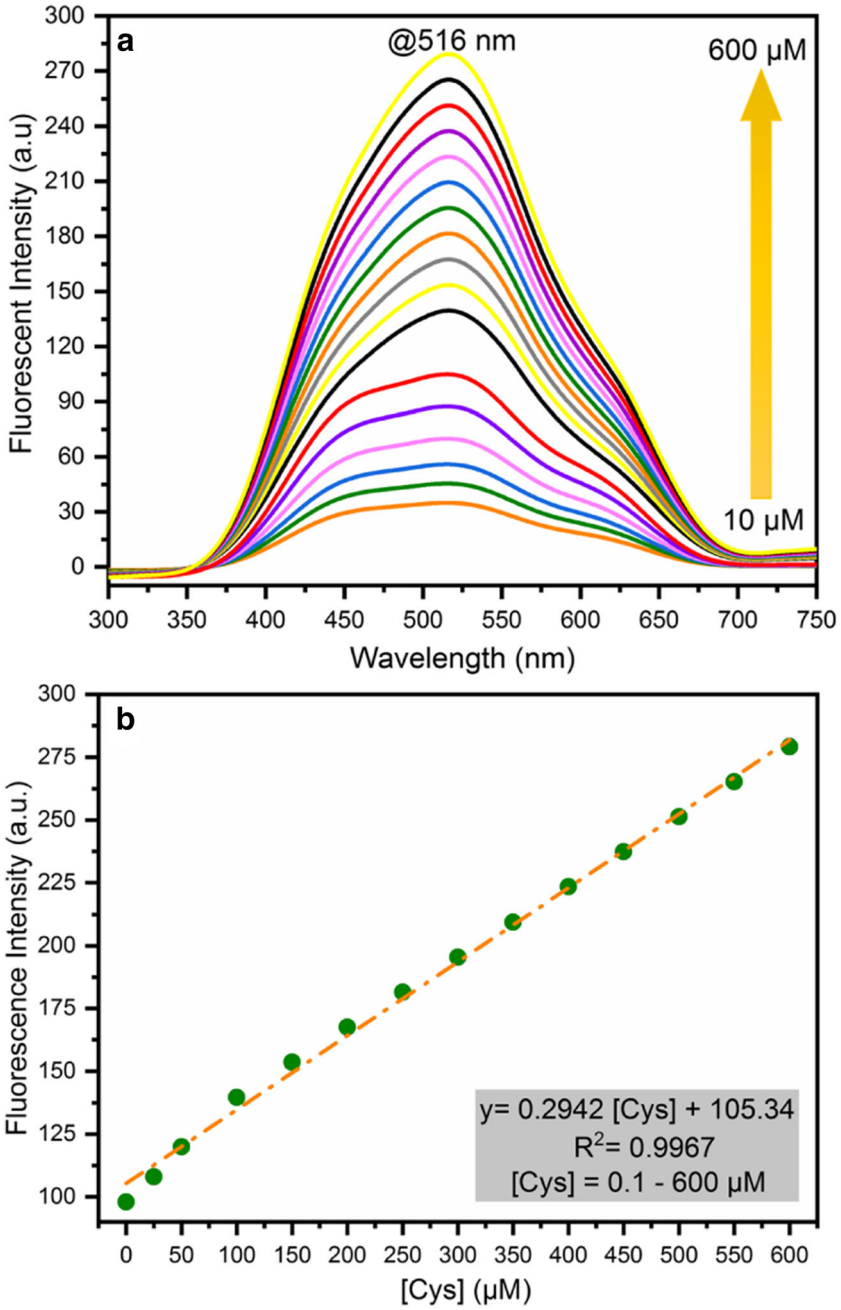

Fig. 7 Cys concentration effect on fluorescent intensity (**a**) and linearity between Cys concentration and fluorescent intensity (**b**)

Conclusion

In this study, a melamine-based fluorescent pre-probe was successfully synthesized, and it was mixed with ZnO quantum dots to prepare the fluorescent probe. The prepared sensor was used for the detection of cysteine in different solutions such as BSA and tap water. The ZnO QDs were synthesized via a sol-gel method and they were characterized by using FT-IR, SEM, XRD techniques, and a nano-particle size analyzer. The average diameter of ZnO QDs was found as 28.03±9.86 or 31.95 ±10.02 nm with nanoparticle size for XRD and analyzer, respectively. The ZnO QDs-based fluorescent biosensor was exhibited a highly selective and strong fluorescence response toward cysteine. The distinction of the emission intensity values between cysteine and the other analytes was still clearly obvious and the interference effect of these analytes such as amino acids, anions, and cations was negligible. The LOD value of the biosensor was found as 0.642 μM, the linear range was determined in the range from 0.1 to 600 μM. The developed sensor was showed a relatively wide linear range compared to the other studies and the LOD value of the biosensor is also comparable with the other studies.

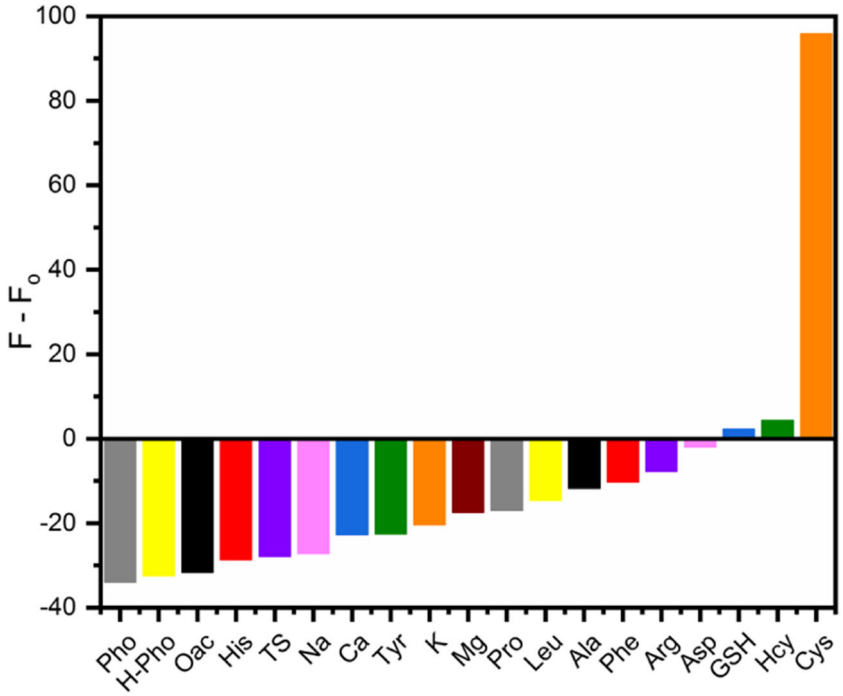

Fig. 8 Interference effect on ZnO quantum dot-based fluorescent sensor for the detection of Cys

Table 1 Comparison of the proposed ZnO quantum dots-based fluorescence probe for the detection of Cys with the other study

Material	Method	LOD	Linear range	References
Lucigenin and carbon QDs	Chemiluminescence	8.8 μM	10–100 μM	49
MoS_2 QDs and Ag NPs	Colorimetric	0.82 μM	1–100 μM	50
CeO_2 NCs	Electrochemical	0.01 μM	0.01–5.0 μM	51
Ag NPs and graphene QDs	Electrochemical	0.01 μM	0.1–200 μM	52
Hydroxyapatite NPs	Fluorometric	0.11 μM	0.2–10 μM	53
Glutathione-Au NCs, Ce (III)	Fluorometric	0.15 μM	0.4–120 μM	32
Carbon QDs and Au NPs	Fluorescence	0.012 μM	0.2–4.0 μM	47
ZnO QDs, SA, and MEL	Fluorescence	0.642 μM	0.1–600 μM	This study

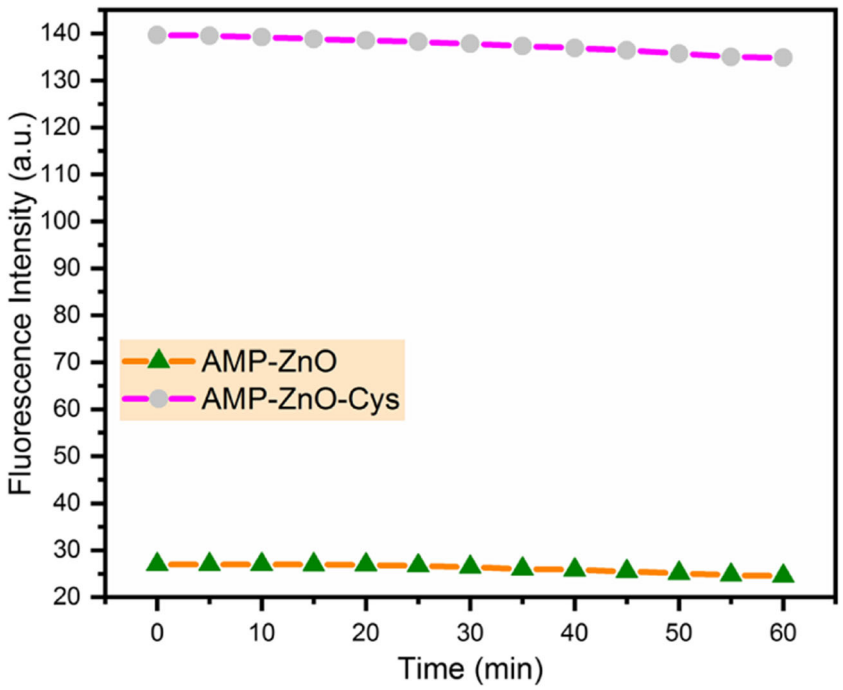

Fig. 9 Photostability of AMP-ZnO QDs and AMP-ZnO-Cys

Table 2 Analytical application of the fluorescent biosensor

Sample	Foreign substance (μL)	Cys added (μL)	Cys founded (μL)	Recovery (%)	Relative Standard Deviation (%)
1	BSA (10)	3.0	2.99	99.7	1.24
3	BSA (300)	3.0	3.02	100.7	2.46
4	BSA (600)	6.0	6.03	100.5	1.17
5	Tap water (10)	3.0	3.04	101.3	1.32
6	Tap water (300)	6.0	6.05	100.8	1.27
2	Tap water (600)	6.0	5.97	99.5	1.38

Availability of Data and Material All data generated or analyzed during this study are included in this published article.

Author's Contributions Umran DURU KAMACI: Conceptualization, Methodology, Formal analysis, Writing. Musa KAMACI: Conceptualization, Investigation, Visualization, Writing - review & editing.

Compliance with Ethical Standards

Conflict of Interest The authors declare that they have no known competing financial interests or personal relationships that could have appeared to influence the work reported in this paper.

References

1. Fonoberov VA, Balandin AA (2006) ZnO quantum dots: Physical properties and optoelectronic applications. J Nanoelectron Optoelectron 1:19–38
2. Gulia S, Kakkar R (2013) ZnO quantum dots for biomedical applications. Adv Mat Lett 4:876–887
3. Udhayakumari D (2020) Detection of toxic fluoride ion via chromogenic and fluorogenic sensing. A comprehensive review of the year 2015–2019. Spectrochim Acta A 228:117817
4. Farshbaf M, Davaran S, Rahimi F, Annabi N, Salehi R, Akbarzadeh A (2018) Carbon quantum dots: recent progresses on synthesis, surface modification and applications. Artif Cell Nanomed B 46: 1331–1348
5. Li Y, Xu X, Wu Y, Zhuang J, Zhang X, Zhang H, Lei B, Hu C, Liu Y (2020) A review on the effects of carbon dots in plant systems. Mater Chem Front 4:437–448
6. Zhao X, Liao S, Wang L, Liu Q, Chen X (2019) Facile green and one-pot synthesis of purple perilla derived carbon quantum dot as a fluorescent sensor for silver ion. Talanta 201:1–8
7. Zou T, Xing X, Yang Y, Wang Z, Wang Z, Zhao R, Zhang X, Wang Y (2020) Water-soluble ZnO quantum dots modified by (3-aminopropyl) triethoxysilane: The promising fluorescent probe for the selective detection of Cu^{2+} ion in drinking water. J Alloys Compd 825:153904
8. Wang C, Shi H, Yang M, Yan Y, Liu E, Ji Z, Fan J (2020a) Facile synthesis of novel carbon quantum dots from biomass waste for highly sensitive detection of iron ions. Mater Res Bull 110730:124
9. Wang C, Shi H, Yang M, Yan Y, Liu E, Ji Z, Fan J (2020b) A novel nitrogen-doped carbon quantum dots as effective fluorescent probes for detecting dopamine. J Photoch Photobio A 391:112374
10. Ge Q, Kong WH, Liu XQ, Wang YM, Wang LF, Ma N, Li Y (2020) Hydroxylated graphene quantum dots as fluorescent probes for sensitive detection of metal ions. Int J Miner Metall Mater 27: 91–99
11. Wang S, Chu X, Xiang X, Cao Y (2020c) Highly selective antenna effect of graphene quantum dots (GQDs): A new fluorescent sensitizer for rare earth element terbium in aqueous media. Talanta 209: 120504
12. Cai L, Zhang Z, Xiao H, Chen S, Fu J (2019) An eco-friendly imprinted polymer based on graphene quantum dots for fluorescent detection of p-nitroaniline. RSC Adv 9:41383–41391
13. Wang Y, Wang Y, Liu H (2019a) A novel fluorescence and spe adsorption nanomaterials of molecularly imprinted polymers based on quantum dot-grafted covalent organic frameworks for the high selectivity and sensitivity detection of ferulic acid. Nanomaterials 9: 305
14. Adegoke O, Pereira-Barros MA, Zolotovskaya S (2020) Aptamer-based cocaine assay using a nanohybrid composed of ZnS/Ag_2Se quantum dots, graphene oxide and gold nanoparticles as a fluorescent probe. Microchim Acta 187:104
15. Zhou ZQ, Liao YP, Yang J, Huang S, Xiao Q, Yang LY, Liu Y (2020) Rapid ratiometric detection of Cd^{2+} based on the formation of ZnSe/CdS quantum dots. Spectrochim Acta A 228:117795
16. Fu H, Hu O, Fan Y, Hu Y, Huang J, Wang Z, She Y (2019) Rational design of an "on-off-on" fluorescent assay for chiral amino acids based on quantum dots and nanoporphyrin. Sens Actuators B Chem 287:1–8
17. Zhang Y, Xiao Y, Zhang Y, Wang Y (2020) Carbon quantum dots as fluorescence turn-off-on probe for detecting Fe^{3+} and ascorbic acid. J Nanosci Nanotechnol 20:3340–3347
18. Ensafi AA, Nasr-Esfahani P, Rezaei B (2017) Quenching-recovery fluorescent biosensor for DNA detection based on mercaptopropionic acid-capped cadmium telluride quantum dots aggregation. Sens Actuators B Chem 249:149–155
19. Liang SS, Qi L, Zhang RL, Jin M, Zhang ZQ (2017) Ratiometric fluorescence biosensor based on CdTe quantum and carbon dots for double strand DNA detection. Sens Actuators B Chem 244:585–590
20. Bano D, Kumar V, Chandra S, Singh VK, Mohan S, Singh DK, Talat M, Hasan SH (2019) Synthesis of highly fluorescent nitrogen-rich carbon quantum dots and their application for the turn-off detection of cobalt (II). Opt Mater 92:311–318
21. Fana L, Wanga Y, Lia L, Zhou J (2020) Carbon quantum dots activated metal organic frameworks for selective detection of Cu(II) and Fe(III). Colloids Surf A Physicochem Eng Asp 124378:588
22. Fakhroueian Z, Vahabpour R, Assmar M, Massiha A, Zahedi A, Esmaeilzadeh P, Katouzian F, Rezaei S, Keyhanvar P, Dehshir AM (2018) ZnO Q-dots as a potent therapeutic nanomedicine for in vitro cytotoxicity evaluation of mouth KB44, breast MCF7, colon HT29 and HeLa cancer cell lines, mouse ear swelling tests in vivo and its side effects using the animal model. Artif Cell Nanomed B 46:96–111
23. Wang X, Xu K, Yan X, Xiao X, Aruta C, Foglietti V, Ning Z, Yang N (2020d) Amorphous ZnO/PbS quantum dots heterojunction for efficient responsivity broadband photodetectors. ACS Appl Mater Interfaces 12:8403–8410
24. Li SH, Mou QQ, Qianqian, Leung PHM (2017a) Synthesis of photoluminescent ZnO quantum dots and its application in bioimaging. Nanosci Nanotech Lett 9:1514–1519
25. Zhang X, Lan W, Xu J, Luo Y, Pan J, Liao C, Yang L, Tan W, Huang X (2019) ZIF-8 derived hierarchical hollow ZnO nanocages with quantum dots for sensitive ethanol gas detection. Sens Actuators B Chem 289:144–152
26. Xu B, Cao Q, Zhang Y, Yu W, Zhu J, Liu D, Jiang G (2018) Microneedles integrated with ZnO quantum-dot-capped mesoporous bioactive glasses for glucose-mediated insulin delivery. Biomater Sci Eng 4:2473–2483
27. Jensen KS, Hansen RE, Winther JR (2009) Kinetic and thermodynamic aspects of cellular thiol–disulfide redox regulation. Antioxid Redox Signal 11:1047–1058
28. Wang XD, Fan L, Ge JY, Li F, Zhang CH, Wang JJ, Shuang SM, Dong C (2019b) A lysosome-targetable fluorescent probe for real-time imaging cysteine under oxidative stress in living cells. Spectrochim Acta A 221:117175
29. Paulsen CE, Carroll KS (2013) Cysteine-mediated redox signaling: Chemistry, biology, and tools for discovery. Chem Rev 113:4633–4679
30. Sun W, Tang X, Li J, He M, Zhang R, Han X, Zhao Y, Ni Z (2020) A novel 4-hydroxypyrene-based "off–on" fluorescent probe with large Stokes shift for detecting cysteine and its application in living cells. Tetrahedron Lett 61:151467
31. Wang JY, Liu ZR, Ren M, Kong X, Lin W (2017) A fast-response two-photon fluorescent probe for the detection of Cys over GSH/

Hcy with a large turn-on signal and its application in living tissues. J Mater Chem B 5:134–138
32. Lai Q, Liu Q, Zhao K, Duan X, Wang G, Su X (2019) Fluorometric determination and intracellular imaging of cysteine by using glutathione capped gold nanoclusters and cerium (III) induced aggregation. Microchim Acta 186:327
33. Duru Kamaci U, Kamaci M, Aysegul P (2019) Poly(azomethine-urethane) and zeolite-based composite: Fluorescent biosensor for DNA detection. Spectrochim Acta A 212:232–239
34. Kamaci M, Kaya I (2016) New low-band gap polyurethanes containing azomethine bonding: Photophysical, electrochemical, thermal and morphological properties. J Taiwan Inst Chem E 59:536–546
35. Kamaci M, Kaya I (2018) Melamine-based poly(azomethine) hydrogels: Mechanical, biodegradability, drug loading and antibacterial properties. Eur Polym J 108:107–115
36. Kaya I, Yıldırım M, Kamaci M (2011) A new kind of optical Mn (II) sensor with high selectivity: Melamine based poly(azomethine-urethane). Synth Met 161:2036–2040
37. Chen Z, Li XX, Du G, Chen N, Suen AYM (2011) A sol–gel method for preparing ZnO quantum dots with strong blue emission. J Lumin 131:2072–2077
38. Hamizi NA, Johan MR, Ghazali N, Wahab YA, Chowdhury ZZ, Akbarzadeh O, Sagadevan S, Badruddin IA, Khan TMY, Kamangar S (2019) Lattice strain analysis of a Mn-doped CdSe QD system using crystallography techniques. Processes 7:639
39. Gutul T, Rusu E, Condur N, Ursaki V, Goncearenco E, Vlazan P (2014) Preparation of poly(*N*-vinylpyrrolidone)-stabilized ZnO colloid nanoparticles. Beilstein J Nanotechnol 5:402–406
40. Vidhya K, Saravanan M, Bhoopathi G, Devarajan VP, Subanya S (2015) Structural and optical characterization of pure and starch-capped ZnO quantum dots and their photocatalytic activity. Appl Nanosci 5:235–243
41. Li L, Liao L, Ding Y, Zeng H (2017b) Dithizone-etched CdTe nanoparticles-based fluorescence sensor for the off–on detection of cadmium ion in aqueous media. RSC Adv 7:10361–10368
42. Pletnev S, Pletneva NV, Souslova EA, Chudakov DM, Lukyanov S, Wlodawer A, Dautera Z, Pletnev V (2012) Structural basis for bathochromic shift of fluorescence in far-red fluorescent proteins eqFP650 and eqFP670. Acta Cryst D68:1088–1097
43. Kamaci M, Kaya I (2015) 2,4-Diamino-6-hydroxypyrimidine based poly(azomethine-urethane): Synthesis and application as a fluorescent probe for detection of Cu^{2+} in aqueous solution. J Fluoresc 25:1339–1349
44. Li M, Zheng K, Chen H, Liu X, Xiao S, Yan J, Tan X, Zhang N (2019) A novel 2,5-bis(benzo[d]thiazol-2-yl)phenol scaffold-based ratiometric fluorescent probe for sensing cysteine in aqueous solution and serum. Spectrochim Acta A 217:1–7
45. Chen Y, Qin X, Yuan C, Wang Y (2020) Switch on fluorescence mode for determination of L-cysteine with carbon quantum dots and Au nanoparticles as a probe. RSC Adv 10:1989–1994
46. Hager G, Brolo AG (2009) Protonation and deprotonation of cysteine and cystine monolayers probed by impedance spectroscopy. J Electroanal Chem 625:109–116
47. Rad GD, Asghari K, Tavallali H (2020) Development of a reversible indicator displacement assay based on the 1-(2-Pyridylazo)-2-naphthol for colorimetric determination of cysteine in biological samples and its application to constructing the paper test strips and a molecular-scale set/reset memorized device. Appl Biochem Biotechnol 192:85–102
48. Kamaci M, Kaya I (2017) A highly selective, sensitive and stable fluorescent chemosensor based on Schiff base and poly(azomethine-urethane) for Fe^{3+} ions. J Ind Eng Chem 46: 234–243
49. Wang C, Lan Y, Yuan F, Fereja TH, Lou B, Han S, Li J, Xu G (2020e) Chemiluminescent determination of L-cysteine with the lucigenin-carbon dot system. Microchim Acta 187:50
50. Li Y, Shen C, Li X, Yang M, Shao C (2018) Hydroxyapatite nanoparticle based fluorometric determination and imaging of cysteine and homocysteine in living cells. Microchim Acta 185:271
51. Manibalan G, Murugadoss G, Thangamuthu R, Kumar MR, Kumar RM (2020) CeO_2-based heterostructure nanocomposite for electrochemical determination of L-cysteine biomolecule. Inorg Chem Commun 113:107793
52. Ojha RP, Mishra R, Singh P, Nirala NR, Prakash R (2020) A composite prepared from MoS_2 quantum dots and silver nanoparticles and stimulated by mercury (II) is a robust oxidase mimetic for use in visual determination of cysteine. Microchim Acta 187:74
53. Yao J, Liu C, Liu L, Chen M, Yang M (2018) An electrochemical sensor for sensitive determination of L-cysteine and its electrochemical kinetics on AgNPs/GQDs/GCE composite modified electrode. J Electrochem Soc 165:B551–B558